

# Kinetics of discontinuous precipitation in a Zn–2.5 at% Cu alloy

I. MANNA, J. N. JHA, S. K. PABI

*Metallurgical Engineering Department, Indian Institute of Technology, Kharagpur, W. B. 721 302, India*

The morphology and growth kinetics of discontinuous precipitation in a Zn–2.5 at% Cu alloy have been studied in the temperature range 383–583 K by optical and scanning electron microscopy. The precipitate phase has a lamellar morphology, and maintains a statistically constant interlamellar spacing under isothermal growth conditions. The interlamellar spacing increases with an increase in temperature. The isothermal growth kinetics in terms of reaction front migration rate is maximum at 523 K. The upper temperature limit for the occurrence of reaction in this alloy has been predicted to be 643 K. A detailed kinetic analysis of the experimental data using several analytical models has confirmed discontinuous precipitation in this system to be a boundary diffusion controlled reaction, and enabled the determination of the grain boundary chemical diffusivity of Cu in a Zn-rich Zn–Cu alloy in the temperature range studied. The corresponding activation energy values determined in this study, range between 65 to 86 kJ/mol<sup>-1</sup>, which compare well with the relevant data in the literature.

## 1. Introduction

Discontinuous precipitation (DP) involves decomposition of a supersaturated matrix phase,  $\alpha_0$ , across a migrating boundary, into a two phase lamellar aggregate comprising a solute depleted matrix,  $\alpha$ , and a precipitate phase,  $\beta$  [1–4]. The migrating boundary provides a short circuit path for solute transport, and hence is called the reaction front (RF) [2–4]. Analysis of the steady state DP reaction kinetics offers a convenient and reliable method of estimating the grain boundary chemical diffusivity triple product,  $s\delta D_b$ , in systems which undergo DP [3]. This approach is particularly useful for the systems in which  $s\delta D_b$  data either do not exist in the literature or are not reliable. Several studies have already been carried out to estimate  $s\delta D_b$  through the kinetic analysis of DP in a number of binary systems, such as Zn–Al [5], Zn–Ag [6, 7], Cu–In [8], Ni–Sn [9], Al–Zn [10], etc. The present paper concerns a similar investigation on the Zn-rich Zn–Cu system.

Smith [11] reported the occurrence of DP in the Zn–Cu system for the first time. In a more detailed study, Watanabe and Koda [12] calculated the activation energy of boundary chemical diffusion,  $Q_b$ , using an empirical relation between the RF velocity,  $v$ , and  $Q_b$ . Subsequently, Abdou and Gust [13] took both  $v$  and interlamellar spacing,  $\lambda$ , into account in the estimation of  $s\delta D_b$  as a function of temperature. However, Abdou and Gust [13] utilized only the analytical model on DP by Petermann and Hornbogen [14] to obtain  $Q_b$ . In the present paper, a detailed microstructural study and kinetic analysis of DP using several analytical models in a Zn–2.5 at% Cu alloy are reported. It may be pointed out that the  $s\delta D_b$  data for

the diffusion of Cu into Zn–Cu does not exist in the literature except for the study by Abdou and Gust [13].

## 2. Experimental procedure

The Zn–Cu alloy containing 2.5 at% Cu was prepared from high purity materials by melting in an Ar atmosphere. The cast ingot (10 mm in diameter) was homogenized at 678 K for 15 days in a similar Ar atmosphere, followed by quenching in water at room temperature. Circular discs of 5 mm thickness were cut from the ingot for metallographic studies. The specimens were solution annealed at 678 K for 14 h, water quenched to room temperature, and then isothermally held (for DP) in the temperature,  $T$ , range 383 to 603 K for different lengths of time,  $t$ , using either an oil bath or a muffle furnace (with samples in Ar-filled glass capsules) controlled to  $\pm 0.5$  K. Samples for metallographic studies were prepared by conventional mechanical polishing using 0.1  $\mu\text{m}$  diamond paste. A colour tinting solution containing 20 g  $\text{Cr}_2\text{O}_3$  and 750 mg  $\text{Na}_2\text{SO}_4$  in 100 ml of distilled water was used for etching the polished samples. While optical microscopy (OM) was utilized to determine the necessary experimental parameters for isothermal growth-kinetic analysis, the morphology and mechanism of the DP colony growth were studied by scanning electron microscopy (SEM). Random measurements of the maximum normal distance between original position of the boundary to its leading edge after DP, obtained from 30–50 different colonies in the microstructure, were used to obtain the average of the maximum DP colony width,  $\bar{w}$ . It may be noted that

the probable error in determining the true colony width,  $w$ , due to the difference in the growth orientation of the DP colonies with respect to the plane of observation was normalized by multiplying  $\bar{w}$  by the correction factor  $\pi/4$  [15]. The isothermal growth rate, expressed by  $v$ , was determined from the slope of the plots of  $w$  as a function of  $t$  at different isothermal conditions. Since the morphology of the precipitate phase,  $\beta$ , was mostly lamellar in nature, similar normalization was also applied to determine the true  $\lambda$ . Finally, X-ray diffraction (XRD) analysis was carried out to estimate the difference in composition between the  $\alpha_0$  and  $\alpha$  phases in the course of DP.

### 3. Results and discussion

#### 3.1. Morphology and distribution of $\beta$ lamellae

Fig. 1 is a typical microstructure showing the decomposition products of DP, consisting of alternate lamellae of  $\alpha$  and  $\beta$  phases. The  $\beta$  lamellae rarely extend to the entire width of the colony, and tend to fragment, either during growth to surface tension forces (tendency of lamellae-spheroidization [16]), or during sample preparation due to mechanical polishing. Interestingly, the lamellar morphology of the DP reaction products observed in this alloy is in contrast with the earlier observation of rod-like morphology of the  $\beta$  phase in the other binary Zn-rich systems, e.g. Zn–Al [5] and Zn–Ag [7] alloys. Usually, the  $\beta$  lamellae are parallel to each other, and are perpendicular to the RF. However, the precise thermodynamic condition and physical constraint in front of the RF may lead to a change in the RF migration direction; and, consequently, also in the orientation of the  $\beta$  lamellae within a DP colony *vis-à-vis* that of the concerned RF (Fig. 2). In general, the DP colonies in the present alloy initiate at grain boundaries of favourable misorientation and curvature [16], and consume the  $\alpha_0$  grains according to the available thermodynamic driving force. However, sharp changes in the direction of RF migration may leave behind a certain area fraction of the  $\alpha_0$  grains untransformed (Fig. 3), which could subsequently undergo continuous or matrix precipitation. Fig. 4 reveals a population of Widman-

statten type of continuous–matrix precipitates in the untransformed  $\alpha_0$  region, especially along the deformation bands introduced during sample preparation by mechanical polishing. This microstructural feature is more common during isothermal precipitation for an extended period of time, especially at  $T \geq 423$  K. The size and volume fraction of these matrix precipitates are found to increase linearly with time. The

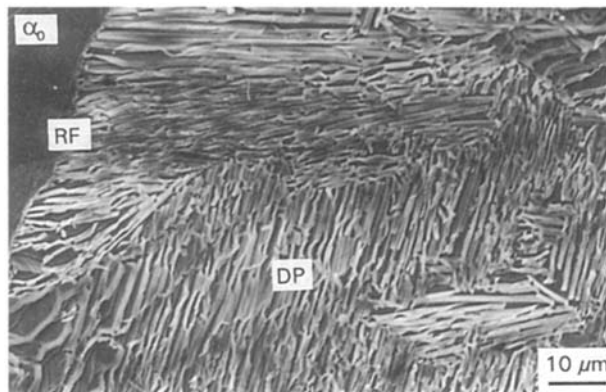


Figure 2 Microstructure revealing a particular stage of growth ( $T = 503$  K,  $t = 2$  h) of a DP colony. The statistically constant distribution of the  $\beta$  lamellae, and the variation of orientation of the  $\beta$  lamellae with respect to the RF are to be noted.

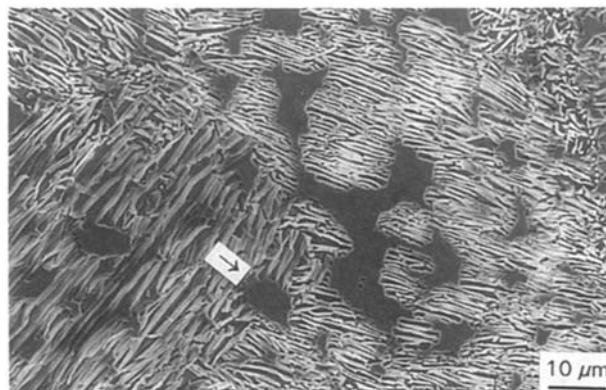


Figure 3 Several untransformed regions of  $\alpha_0$  remaining in the microstructure after DP at 503 K for 2 h (shown by arrowhead).

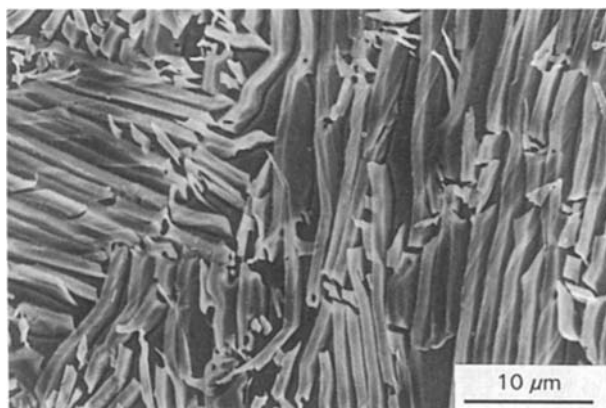


Figure 1 Lamellar decomposition products of DP, following isothermal precipitation at 503 K for 2 h.

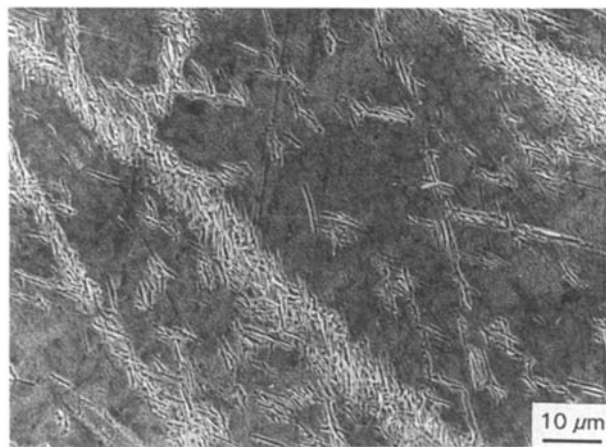


Figure 4 Widmanstatten type of continuous–matrix precipitates in the untransformed  $\alpha_0$  matrix, especially along the deformation bands ( $T = 523$  K,  $t = 45$  min).

presence of a similar matrix precipitate has earlier been reported in other Zn-rich alloys showing DP, e.g. in Zn-Al [5] and Zn-Ag [6]. Finally, it may be pointed out that growth of a DP colony from different segments of the same grain boundary seems to be influenced by the local curvature of the grain boundary, due to which both single and double seam morphology of the growth front [1] has been observed.

During the course of isothermal precipitation, the  $\beta$  phase appears to maintain a statistically constant value of  $\lambda$ , either by repeated nucleation of  $\beta$  along the RF, or by branching of some of the existing  $\beta$  lamellae (Fig. 2).  $\lambda$  increases with an increase in  $T$  (Fig. 5). Extrapolation of the  $1/\lambda$  versus  $T$  plot to  $1/\lambda = 0$  in Fig. 5 yields an X-axis intercept of  $T_{DP} = 643$  K, where  $T_{DP}$  is the highest temperature above which the available chemical driving force is inadequate for supporting the creation of the  $\alpha$ - $\beta$  interfaces and migration of the RF [17]. It may be pointed out that  $T_{DP}$  corresponds to the hypothetical situation where  $\lambda$  is infinite, signifying cessation of DP at  $T \geq T_{DP}$ . It may further be noted that  $T_{DP}$  is marginally lower than the equilibrium solvus temperature ( $T_{SV} = 668$  K) in the present alloy, as was the case with  $T_{DP}$  in the Zn-Ag alloy [7].

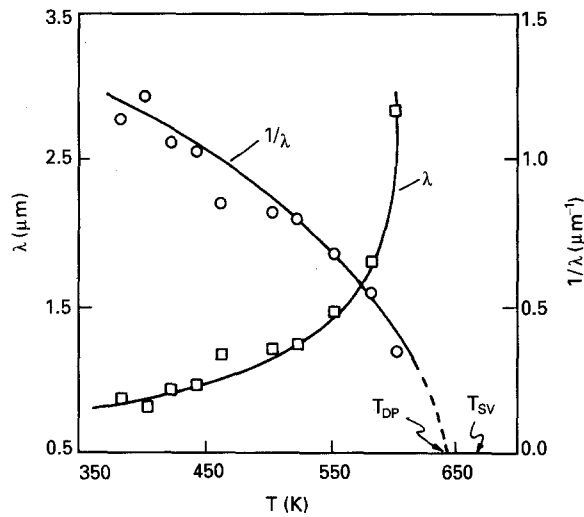


Figure 5 Variation of the interlamellar spacing,  $\lambda$ , and its reciprocal,  $1/\lambda$ , with ageing temperature,  $T$ . Note that  $T_{DP} = 643$  K is less than  $T_{SV} = 668$  K (see text).

### 3.2. Variation of $v$

Fig. 6a,b records the isothermal variation of  $w$  as a function of  $t$  at different  $T$ . A good fit of the respective set of data points for each  $T$  within the time period studied allows determination of  $v = (dw/dt)_T$ , by suitable regression analysis. Table I summarizes the

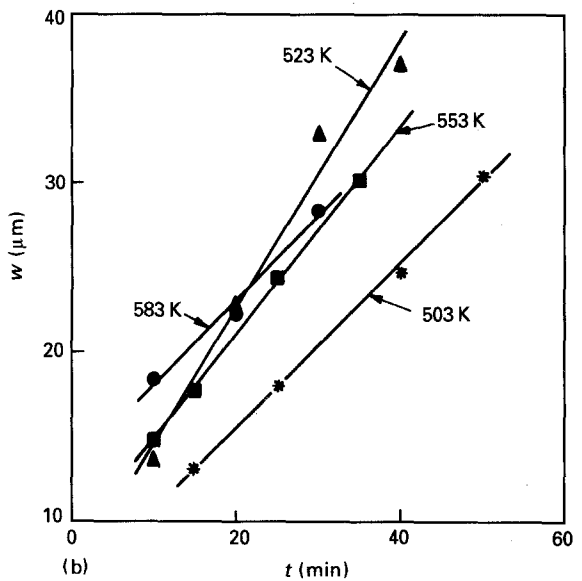
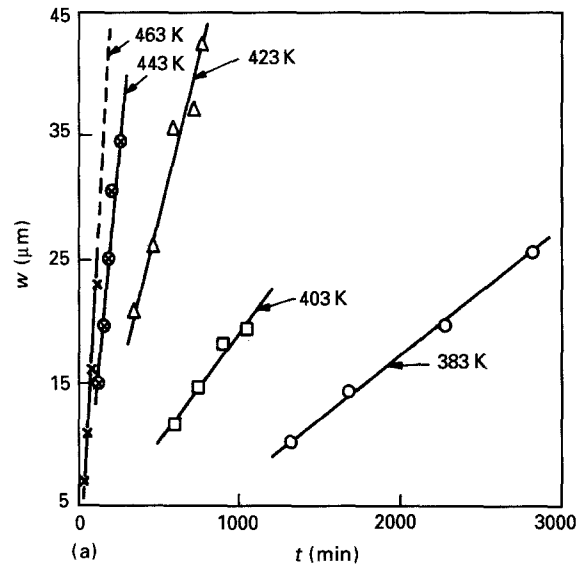


Figure 6 Variation of the DP colony width,  $w$ , as a function of time,  $t$ , at different isothermal conditions: (a) 383–463 K, and (b) 503–583 K.

TABLE I Kinetic and thermodynamic data for DP at different  $T$

$T$ (K)	$\lambda$ ( $\mu\text{m}$ )	$v$ ( $10^{-10} \text{ m s}^{-1}$ )	$X_\alpha$	$X_\beta$	$-\Delta G_c$ ( $\text{J mol}^{-1}$ )	$\gamma$ ( $\text{mJ m}^{-2}$ )	$\Delta G_\gamma$ ( $\text{J mol}^{-1}$ )	$-\Delta G$ ( $\text{J mol}^{-1}$ )
383	0.88	1.7	0.0037	0.139	84.9	299	6.1	78.8
403	0.82	3.7	0.0048	0.139	71.1	297	6.5	64.6
423	0.94	8.4	0.0060	0.139	59.2	295	5.6	53.6
443	0.97	28.5	0.0073	0.139	48.7	293	5.4	43.3
463	1.18	35.0	0.0085	0.139	40.8	291	4.4	36.4
503	1.22	81.7	0.0112	0.137	26.6	287	4.2	22.4
523	1.25	160.7	0.0126	0.137	20.9	285	4.1	16.8
553	1.47	103.3	0.0152	0.137	12.3	282	3.4	8.9
583	1.81	83.0	0.0176	0.137	6.8	279	2.8	4.0
603	2.83	—	—	—	—	—	—	—

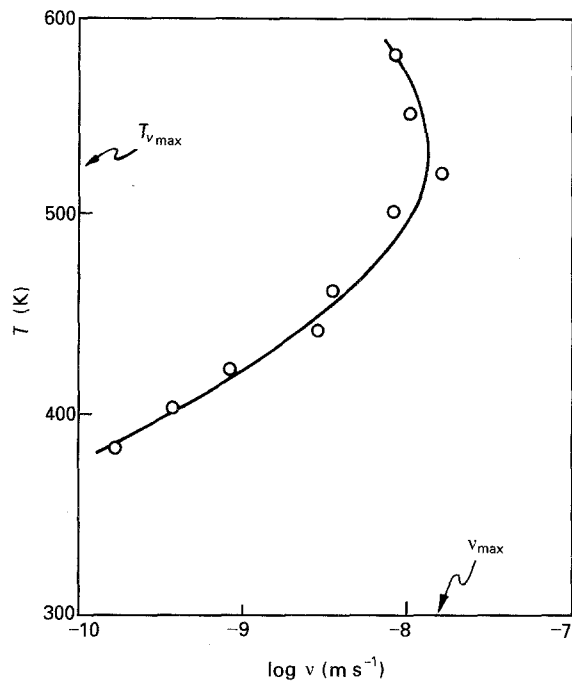


Figure 7 Variation of the RF migration velocity,  $v$ , as a function of isothermal precipitation temperature,  $T$ . Note that  $v_{\max}$  corresponds to  $T_{v(\max)} = 523$  K (see text).

kinetic data for  $v$  as a function of  $T$ . The variation of  $v$  with  $T$  exhibits typical "C-curve" behaviour (Fig. 7). Initially,  $v$  increases by about two orders of magnitude with an increase in  $T$  from 383 to 523 K, and then it decreases above 523 K. The decrease in  $v$  above 523 K may arise due to the decrease in the available chemical driving force near  $T_{sv}$ . It has earlier been suggested that the maximum growth rate,  $v_{\max}$ , in DP occurs at  $T_{v(\max)} = (0.89 \pm 0.04)T_{sv}$  [18]. In the present alloy,  $v_{\max}$  is recorded at  $T_{v(\max)} = 523$  K  $= 0.8T_{sv}$  (Fig. 7). This small difference may be attributed to the strong tendency of continuous-matrix precipitation in the present alloy at higher  $T$  (cf. Fig. 4).

### 3.3. DP growth kinetic analysis

Since the earliest effort by Zener [19] in carrying out a quantitative analysis of the growth kinetics of a moving boundary reaction, a number of analytical models on the kinetics of DP [14, 20–25] have been proposed in the past. In general, these models assume DP to be a boundary diffusion controlled process and express the boundary diffusivity,  $D_b$ , in terms of  $v$  and  $\lambda$  through the following equation

$$s\delta D_b = kv\lambda^2 \quad (1)$$

where  $s$  is the segregation factor [26],  $\delta$  is the grain boundary width, and  $k$  is related to the fraction of supersaturation relieved after DP ( $k$  assumes different forms in the different models). Several of these models [22–25] necessitate the metastable solvus data for the  $\alpha$  phase to calculate a relevant thermodynamic function. Unfortunately, neither the metastable solvus curve for the Zn–Cu system is reported in the literature, nor does X-ray diffraction analysis in the present study evidence a measurable residual solute supersaturation in the  $\alpha$  phase following DP. Therefore,

kinetic analyses in the present study to calculate  $s\delta D_b$  have been carried out only through the models of Turnbull [20], Aaronson and Liu [21] and Petermann and Hornbogen [14], which do not require the metastable solvus data.

The value of the parameter  $k$  for the Turnbull model [20] is as follows

$$k = X_\alpha^o / (X_\alpha^o - X_\alpha^e) \quad (2)$$

where  $X_\alpha^o$  and  $X_\alpha^e$  are the equilibrium solute contents in  $\alpha_0$  and  $\alpha$  phases, respectively.

According to the Aaronson and Liu model [21],  $k$  in Equation 1 is given by

$$k = (X_\beta^e - X_\alpha^o) / [4(X_\beta^e - X_\alpha^e)] \quad (3)$$

where  $X_\beta^e$  is the equilibrium solute content in the  $\beta$  phase.

The expression for  $k$  in the Petermann and Hornbogen model [14] on DP assumes the form

$$k = RT / [8(-\Delta G)] \quad (4)$$

In Equation 4,  $\Delta G$  refers to the total driving force for the DP reaction in terms of the change in the overall Gibbs free energy, and  $R$  is the universal gas constant.  $\Delta G$  comprises two components

$$\Delta G = \Delta G_c + \Delta G_\gamma \quad (5)$$

where  $\Delta G_c$  is the chemical free energy available for the growth of a DP cell, and  $\Delta G_\gamma$  is the interfacial free energy. Since the free energy of formation of the  $\beta$  phase and the activity coefficient of Cu in the concerned phases are not available in the literature,  $\Delta G_c$  may be calculated using the ideal solution model [2] as follows

$$\Delta G_c = -RT \{ X_\alpha^o \ln(X_\alpha^o / X_\alpha^e) + (1 - X_\alpha^o) \ln[(1 - X_\alpha^o) / (1 - X_\alpha^e)] \} \quad (6)$$

Values of  $X_\alpha^e$  and  $X_\beta^e$  in the above expressions are readily obtained from the relevant equilibrium phase diagram [27].

$\Delta G_\gamma$  is obtained from the following expression [22]

$$\Delta G_\gamma = (2\gamma V_m) / \lambda \quad (7)$$

where  $\gamma$  is the interfacial energy per unit area of the  $\alpha/\beta$  boundary, and  $V_m$  denotes the molar volume of the  $\alpha_0$  phase. Since  $\gamma$  for the Zn–Cu system is not available in the literature, and the grain boundary specific energy of pure Zn is  $340$  mJ m $^{-2}$  at  $573$  K [28], it may be reasonable to assume that  $\gamma = 280$  mJ m $^{-2}$  at  $573$  K with  $d\gamma/dT = -0.1$  mJ m $^{-2}$  K $^{-1}$  for the Zn–2.5% Cu alloy (considering a decrease in  $\gamma$  due to alloying). The  $V_m$  value for  $\alpha_0$  in the present alloy has been calculated to be  $8.93 \times 10^{-6}$  m $^3$  mol $^{-1}$ . Thus, the overall change in  $\Delta G$  may be calculated through Equation 5, obtaining  $\Delta G_c$  and  $\Delta G_\gamma$  contributions from Equations 6 and 7, respectively. Fig. 8 illustrates the calculation of  $\Delta G$  from the respective contributions of  $\Delta G_c$  and  $\Delta G_\gamma$  at the concerned isothermal  $T$ . Table I summarizes the necessary thermodynamic data and the calculated values of the free energy changes at the concerned  $T$ , as per Equations 6 and 7, respectively. The values of

$k$  and  $s\delta D_b$ , as per the models of Turnbull [20], Aaronson and Liu [21] and Petermann and Hornbogen [14], obtained from the respective Equations 2, 3 and 4, are listed out in Table II.

### 3.4. Determination of Arrhenius parameters for boundary diffusivity

The temperature dependence of  $s\delta D_b$  is typically expressed through an Arrhenius type of equation as follows

$$s\delta D_b = (s\delta D_b)_0 \exp(-Q_b/RT) \quad (8)$$

where  $(s\delta D_b)_0$  is the preexponential constant. Fig. 9 records the Arrhenius plot of  $s\delta D_b$  derived using the different models on DP [14, 20, 21]. The values of  $(s\delta D_b)_0$  and  $Q_b$  have been determined from the intercept and slope of the straight lines fitted to the  $s\delta D_b$  data, respectively (Fig. 9).

Unlike the analytical models [14, 20–25] discussed so far, Sundquist [29] has proposed the following

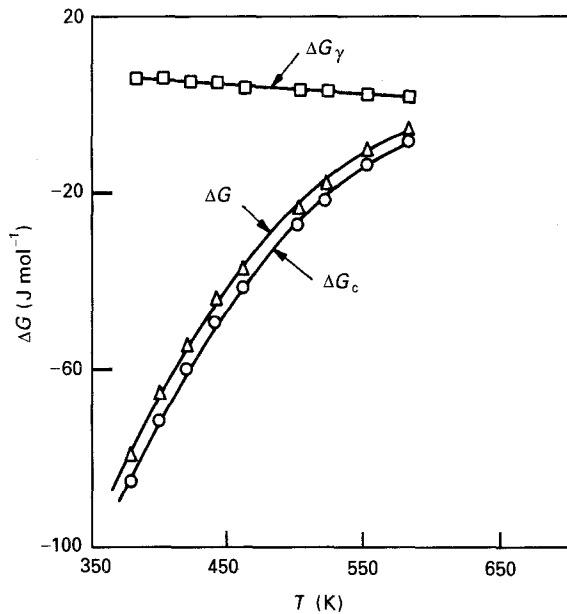


Figure 8 Temperature,  $T$ , dependence of the overall Gibbs free energy change,  $\Delta G$ , with its chemical,  $\Delta G_c$ , and interfacial,  $\Delta G_\gamma$ , contributions for DP in the present alloy.

equation for the interfacial diffusion controlled growth of lamellar cells

$$v/(\Delta T)^3 \approx \exp(-Q_b/RT) \quad (9)$$

where  $\Delta T = (T_{sv} - T)$ . This equation allows direct determination of  $Q_b$  as functions of  $v$  and  $\Delta T$  from the slope of the plots of  $v/(\Delta T)^3$  against the reciprocal of  $T$  (Fig. 9).

Table III summarizes the Arrhenius parameters obtained in the present study using different analytical models [14, 20, 21, 29], and compares them with the relevant data reported in the literature.  $Q_b$  determined using the models by Turnbull [20] and Aaronson and Liu [21] are close to each other, whereas the same using the Petermann and Hornbogen model [14] is relatively higher. However,  $Q_b$  obtained from the Sundquist model [29] lies in between the above values. In general, these values are comparable to the  $Q_b$  for grain boundary self diffusion in Zn [30], and are nearly 0.5–0.7 of that for tracer impurity diffusion of  $\text{Cu}^{64}$  in Zn [31]. It may be noted that the activation energy for volume–bulk diffusion of Cu in Zn-rich Zn–Cu alloy is not available in the literature.

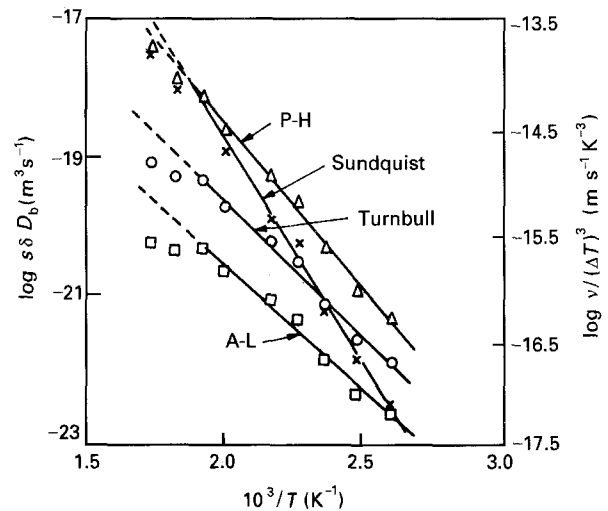


Figure 9 Arrhenius plots of  $s\delta D_b$  by Turnbull [20], Aaronson and Liu (A-L) [21] and Petermann and Hornbogen (P-H) [14] models, and the similar plot of  $v/(\Delta T)^3$  by Sundquist [29] model.

TABLE II The dimensionless thermodynamic parameter,  $k$  (cf. Equation 1), and grain boundary chemical diffusivity,  $s\delta D_b$ , data obtained by different models

$T$ (K)	Turnbull [20]		Aaronson and Liu [21]		Petermann and Hornbogen [14]	
	$k$	$s\delta D_b$ ( $\text{m}^3 \text{s}^{-1}$ )	$k$	$s\delta D_b$ ( $\text{m}^3 \text{s}^{-1}$ )	$k$	$s\delta D_b$ ( $\text{m}^3 \text{s}^{-1}$ )
383	1.17	$1.5 \times 10^{-22}$	0.211	$2.8 \times 10^{-23}$	5.04	$6.6 \times 10^{-22}$
403	1.24	$3.1 \times 10^{-22}$	0.212	$5.3 \times 10^{-23}$	6.47	$1.6 \times 10^{-21}$
423	1.32	$9.8 \times 10^{-22}$	0.214	$1.6 \times 10^{-22}$	8.19	$6.1 \times 10^{-21}$
443	1.41	$3.8 \times 10^{-21}$	0.216	$5.8 \times 10^{-22}$	10.61	$2.8 \times 10^{-20}$
463	1.52	$7.4 \times 10^{-21}$	0.218	$1.1 \times 10^{-21}$	13.20	$6.4 \times 10^{-20}$
503	1.81	$2.2 \times 10^{-20}$	0.222	$2.7 \times 10^{-21}$	23.30	$2.8 \times 10^{-19}$
523	2.02	$5.1 \times 10^{-20}$	0.225	$5.6 \times 10^{-21}$	32.30	$8.1 \times 10^{-19}$
553	2.55	$5.7 \times 10^{-20}$	0.230	$5.1 \times 10^{-21}$	64.46	$1.4 \times 10^{-18}$
583	3.38	$9.2 \times 10^{-20}$	0.234	$6.4 \times 10^{-21}$	151.22	$4.1 \times 10^{-18}$

TABLE III Comparison of the activation energy values for grain boundary chemical diffusion obtained in this study using different models, with relevant data from the literature

Alloy	Grain boundary chemical diffusion				Boundary self diffusion of Zn [30]	Tracer diffusion of Cu <sup>64</sup> in Zn [31]
	T <sup>a</sup> [20]	A-L <sup>a</sup> [21]	P-H <sup>a</sup> [14]	S <sup>a</sup> [29]		
Zn-2.5 Cu <sup>b</sup>	70.5	64.6	85.8	77.4		
Zn-1.8 Al <sup>c</sup>	20.8	20.4	21.6	21.2		
Zn-2.0 Al <sup>c</sup>	25.6	25.6	26.0	21.8	61.1	
Zn-2.0 Ag <sup>d</sup>	58.5	50.3	78.2	57.2		
Zn-4.0 Ag <sup>e</sup>	54.3	48.4	69.0	59.2		

<sup>b</sup>This study. <sup>c</sup>Unpublished data. <sup>d</sup>Data from [7]. <sup>e</sup>Data from [6].

<sup>a</sup>T, Turnbull; A-L, Aaronson and Liu; P-H, Petermann and Hornbogen; S, Sundquist.

#### 4. Conclusions

The Zn-2.5 at % Cu alloy undergoes DP at all temperatures within the range 383–583 K. Matrix continuous precipitation accompanies DP at  $T \geq 423$  K. The precipitate phase maintains a lamellar morphology and a statistically constant interlamellar spacing under the isothermal growth conditions. The interlamellar spacing increases with an increase in isothermal temperature. The RF velocity of the DP colonies shows a typical “C-curve” behaviour. The highest velocity,  $v_{\max}$ , which occurs at  $T_{v(\max)} = 523$  K, is nearly two orders of magnitude higher than that obtained at the lowest temperature studied (383 K). The upper limit of DP,  $T_{DP} = 643$  K, is marginally lower than the solvus temperature,  $T_{SV} = 668$  K. The activation energy values for grain boundary diffusion of Cu in the present Zn-Cu alloy, determined through the models of Turnbull, Aaronson and Liu, Petermann and Hornbogen and Sundquist, vary from 65 to 86 kJ mol<sup>-1</sup>. These values compared well with the same for grain boundary diffusion of Ag or Al in other Zn-base systems, and are significantly lower than that for the tracer (volume) diffusion of Cu in Zn. Therefore, solute transport in DP in the Zn-Cu system seems to occur through the boundaries, and not through the volume-matrix.

#### Acknowledgements

The authors are grateful to Professor W. Gust, Max-Planck-Inst. für Metallforschung, Stuttgart for useful suggestions, and for providing some important unpublished data. Financial support from the Council of Scientific and Industrial Research, India (Grant No. 10-147-91, EMR II), and equipment support from BRNS, DAE, India (Project No. 34/7/89-G) are also acknowledged.

#### References

1. D. B. WILLIAMS and E. P. BUTLER, *Int. Met. Rev.* **26** (1981) 153.
2. W. GUST, in “Phase Transformations”, Series 3, No. 11, Vol 1, edited by The Institute of Metallurgists (The Chameleon Press, London, 1979) p. II/27.

3. M. FRIESEL, I. MANNA and W. GUST, *Colloque de Physique* **51** (1990) C1-381.
4. I. KAUR and W. GUST, in “Fundamental of Grain and Interphase Boundary Diffusion”, 2nd Edn (Ziegler Press, Stuttgart, 1989) p. 222.
5. I. MANNA, W. GUST and B. PREDEL, *Scripta Metall. Mater.* **24** (1990) 1635.
6. I. MANNA, J. N. JHA and S. K. PABI, *Acta Metall. Mater.* (communicated).
7. *Idem*, *Scripta Metall. Mater.* **29** (1993) 817.
8. B. PREDEL and W. GUST, *Mater. Sci. Engng* **16** (1974) 239.
9. S. P. GUPTA, *Acta Metall.* **35** (1987) 747.
10. C. P. JU and R. A. FOURNELLE, *ibid.* **33** (1985) 71.
11. C. S. SMITH, *Trans. Amer. Soc. Met.* **45** (1953) 553.
12. R. WATANABE and S. KODA, *Trans. National Res. Inst. Met.* **7** (1965) 13.
13. S. ABDOU and W. GUST, in “Developments in Production Engineering Design and Control”, edited by A. E. Al-Ashram and M. W. Badawi (Alexandria University, 1989) p. 137.
14. J. PETERMANN and E. HORNBOGEN, *Z. Metallk.* **59** (1968) 814.
15. K. LUCKE, *ibid.* **52** (1961) 1.
16. I. MANNA, S. K. PABI and W. GUST, *Acta Metall. Mater.* **39** (1991) 1489.
17. M. HILLERT, in “Mechanism of Phase Transformation in Crystalline Solids” edited by the Institute of Metals, (London, 1969) p. 231.
18. W. GUST, T. H. CHUANG and B. PREDEL, in “Decomposition of alloys: the early stages”, edited by P. Haasen *et al.* (Pergamon Press, Oxford, 1984) p. 208.
19. C. ZENER, *Trans. AIME* **167** (1946) 550.
20. D. TURNBULL, *Acta Metall.* **3** (1955) 55.
21. H. I. AARONSON and Y. C. LIU, *Scripta Metall.* **2** (1968) 1.
22. J. W. CAHN, *Acta Metall.* **7** (1959) 18.
23. J. M. SHAPIRO and J. S. KIRKALDY, *ibid.* **16** (1968) 1239.
24. B. E. SUNDQUIST, *Metall. Trans.* **A4** (1973) 1919.
25. M. HILLERT, *Acta Metall.* **30** (1982) 1689.
26. G. B. GIBBS, *Phys. Status Solidi* **16** (1966) K27.
27. M. HANSEN and K. ANDERKO, in “Constitution of Binary Alloys” (McGraw-Hill, New York, 1958) p. 649.
28. L. E. MURR, in “Interfacial Phenomena in Metals and Alloys” (Addison-Wesley, London, 1975) p. 133.
29. B. E. SUNDQUIST, *Acta Metall.* **16** (1968) 1413.
30. D. BERGNER and W. LANGE, *Phys. Status Solidi* **18** (1966) 75.
31. C. J. SMITHELLS (Ed.), in “Metals Reference Book” (Butterworth, London, 1976) p. 880.

Received 8 April  
and accepted 6 July 1994